arXiv:1003.0016v1 [astro-ph.CO] 26 Feb 2010

To appear in the ApJ letters

Ionization near-zones associated with quasars at $z \sim 6$

C.L. Carilli[1], Ran Wang[1,2], X. Fan[3], F. Walter[4], J. Kurk[4], D. Riechers[5], J. Wagg[6], J. Hennawi[4], L. Jiang[3], K.M.Menten[7], F. Bertoldi[8], Michael A. Strauss[9], P. Cox[10]

ccarilli@aoc.nrao.edu

ABSTRACT

We analyze the size evolution of HII regions around 27 quasars between $z =$ 5.7 to 6.4 ('quasar near-zones' or NZ). We include more sources than previous studies, and we use more accurate redshifts for the host galaxies, with 8 CO molecular line redshifts and 9 MgII redshifts. We confirm the trend for an increase in NZ size with decreasing redshift, with the luminosity normalized proper size evolving as: $R_{NZ,corrected} = (7.4 \pm 0.3) - (8.0 \pm 1.1) \times (z - 6)$ Mpc. While derivation of the absolute neutral fraction remains difficult with this technique, the evolution of the NZ sizes suggests a decrease in the neutral fraction of intergalactic hydrogen by a factor ~ 9.4 from $z = 6.4$ to 5.7, in its simplest interpretation. Alternatively,

---

⋆The Very Large Array of the National Radio Astronomy Observatory, is a facility of the National Science Foundation operated under cooperative agreement by Associated Universities, Inc

[1]National Radio Astronomy Observatory, P. O. Box 0, Socorro, NM 87801

[2]Purple Mountain Observatory, CAS 2, West Beijing Road, Nanjing, China, 210008

[3]Steward Observatory, University of Arizona, Tucson, AZ, USA, 85721

[4]Max-Planck Institute for Astronomy, Königstuhl 17, 69117, Heidelberg, Germany

[5]Department of Astronomy, California Institute of Technology, MC 249-17, 1200 East California Boulevard, Pasadena, CA 91125, USA; Hubble Fellow

[6]ESO-ALMA, Alonso de Cordova 3107 Vitacura Casilla 19001 Santiago 19, Chile

[7]Max-Planck Institute for Radio Astronomy, Auf dem Hügel 49, Bonn, Germany

[8]Argelander Institute for Astronomy, University of Bonn, Auf dem Hügel 71, 53121 Bonn, Germany

[9]Princeton University Observatory, Peyton Hall, Princeton, NJ 08544, USA

[10]Institut de Radioastronomie Millimetrique, 300 rue de la Piscine, 38406 Saint Martin d'Heres, France

recent numerical simulations suggest that this rapid increase in near-zone size from $z = 6.4$ to 5.7 is due to the rapid increase in the background photo-ionization rate at the end of the percolation or overlap phase, when the average mean free path of ionizing photons increases dramatically. In either case, the results are consistent with the idea that $z \sim 6$ to 7 corresponds to the tail end of cosmic reionization. The scatter in the normalized NZ sizes is larger than expected simply from measurement errors, and likely reflects intrinsic differences in the quasars or their environments. We find that the near-zone sizes increase with quasar UV luminosity, as expected for photo-ionization dominated by quasar radiation.

Subject headings: cosmology: theory, reionization - galaxies: formation - quasars: formation

1. Introduction

Observations have set the first constraints on the epoch of reionization (EoR), corresponding to the formation epoch of the first luminous objects (see the review by Fan, Carilli, & Keating 2006a). Studies of Gunn-Peterson (GP) absorption in quasar spectra (Gunn & Peterson 1965), and related phenomena, suggest a qualitative change in the state of the intergalactic medium (IGM) at $z \sim 6$, indicating a rapid increase in the neutral fraction of the IGM, from f(HI) $< 10^{-4}$ at $z \leq 5.5$, to f(HI) $> 10^{-3}$ (by volume) at $z \geq 6$. Conversely, the large scale polarization of the cosmic microwave background (CMB) is consistent with instantaneous reionization at $z \sim 10.4 \pm 1.2$ (Komatsu et al. 2010). These data suggest that reionization is less an event than a process, beginning at $z \geq 10$, and with the 'percolation', or 'bubble overlap' phase ending at $z \sim 6$ to 7. Unfortunately, current methods for measuring the neutral fraction of the IGM have fundamental limitations, as GP absorption saturates at low neutral fractions (f(HI) $> 10^{-3}$), and CMB polarization measurements are an integral measure of the Thompson scattering optical depth back to $z = 1000$. Indeed, Mesinger (2010) has pointed out that there is no definitive evidence for (or against) a largely ionized IGM, even as late as $z \sim 6$, while recent measurements of the temperature of the high z Lyα forest suggest fairly late reionization ($z < 9$; Bolton et al. 2010).

Luminous quasars at the end of cosmic reionization will generate the largest ionized regions in the Universe during this epoch. These have been alternatively called Cosmological Strömgren Spheres or quasar near-zones (NZ), and we adopt the latter to be consistent with the recent literature. The near-zone behavior has been described by numerous authors (Shapiro & Giroux 1987; Madau & Rees 2000; Cen & Haiman 2000). A straight-forward

calculation (Haiman 2002) shows that, when recombination is not important, and when the quasar lifetime is much less than the age of the Universe, the physical size of the expected NZ behaves as:

$$R_{NZ} = 8.0\ f(HI)^{-1/3}(\dot{N}_Q/6.5\times10^{57}s^{-1})^{1/3}(t_Q/2\times10^7 yr)^{1/3}[(1+z_Q)/7]^{-1}Mpc$$

where R_{NZ} is the NZ proper radius, $\dot{N}_Q$ is the rate of ionizing photons from the quasar, z_Q is the quasar host galaxy redshift[1], and t_Q is the quasar age. This calculation ignores clumping, and assumes the mean cosmic density over the large scales being considered.

Spectra of $z \sim 6$ quasars show evidence for large ionized regions around bright quasars on proper scales ~ 5 Mpc. The evidence comes in the form of excess transmission on the blue wing of the Lyα emission line, prior to the onset of full GP absorption. This excess emission has been interpreted as being due to the local ionizing effect of the quasar. A number of studies have attempted to use these NZ to derive constraints on the IGM neutral fraction, using the equation above and assuming mean quasar lifetimes derived from demographics (White et al. 2003, 2005; Mesinger & Haiman 2004; Wyithe, Loeb, & Carilli 2005; Yu & Lu 2005; Gnedin & Prada 2004; Furlanetto, Hernquist & Zaldariaga 2004; Wyithe & Loeb 2004; Walter et al. 2003).

The most detailed treatment of quasar near-zones associated with $z \sim 6$ quasars to date is that by Fan et al. (2006b). They point out numerous factors that make the absolute measurement of the neutral fraction using NZ radii difficult, including: (i) uncertainties in the mean quasar lifetimes and ionizing photon rates, (ii) large scale structure in biased regions and pre-ionization by local galaxies, and (iii) clumpiness in the IGM (see also Lidz et al. 2007; Maselli et al. 2007; Bolton & Heahnelt 2007a,b). However, Fan et al. also point out that over the narrow redshift range being considered, the systematics are likely to be comparable for all sources, and hence, 'if there is an order of magnitude evolution in the IGM ionization, the size of the HII regions should show strong evolution, providing a reliable *relative* measurement of the neutral fraction (with redshift).'

More recently, Wyithe et al. (2008) and Bolton et al. (2010) have argued, based on numerical simulations, that the dominant effect on quasar near-zones during the end of reionization, or the percolation stage, when the overall neutral fraction is low, may be a rapidly increasing contribution to photo-ionization from the cosmic ionizing background with cosmic time, acting in concert with the quasar photons to lift the GP trough near the

[1]Note that we make the reasonable assumption that the quasar is at rest relative to its host galaxy.

edge of the near-zone.

Fan et al. (2006b) emphasize that the measurements of the NZ sizes are uncertain due to a number of factors, including the determination of where the transmission drops to zero, ie. the on-set of the GP effect (z_{GP}), and the redshift of the host galaxy (z_Q). To mitigate the former, they define the ionization zone, R_{NZ}, as the region in which the transmitted flux ratio (relative to the extrapolated continuum) is above 0.1 when smoothed to a resolution of 20 $\mathring{A}$. This is well above the average GP transmission for quasars at this redshift (< 0.04), and hence mitigates affects of a fluctuating IGM, while still providing a good relative measurement of NZ sizes over the narrow redshift range considered. Willott et al. (2008) have considered this technique for two $z \sim 6$ quasars, and point out that the transmission can rise above 0.1 just one or two resolution elements further from the quasar, raising the question of where to draw the line for R_{NZ}? In this paper, we use the strict and quantifiable definition of Fan et al. (2006b), namely, the first redshift below the quasar redshift at which the transmission drops under 0.1, in order to be consistent with previous literature. We refer the reader to the extensive discussion in Fan et al. 2006b and Willott et al. (2008) for details.

One major uncertainty in the Fan et al. (2006b) analysis was the host galaxy redshift, z_Q. In particular, most of the host galaxy redshifts in the Fan et al. sample were based on a combination of Lyα+NV and high-ionization lines such as CIV and Si IV. It is well documented that broad Lyα emission is a poor indicator of the host galaxy redshift due to absorption on the blue-side of the emission line, while the high ionization lines can have large velocity offsets, of order 1000 km s^{-1} ($\Delta z \sim 0.02$ at $z = 6$), with respect to low ionization lines such as MgII (Richards et al. 2002).

We have undertaken an extensive study of the radio through submm properties of $z > 5.7$ quasars to probe the dust, molecular gas, and star formation properties of the host galaxies (Wang et al. 2010; Wang et al. 2008; Wang et al. 2007; Carilli et al. 2007; Walter et al. 2009; Walter et al. 2004; Bertoldi et al. 2003; Bertoldi et al. 2003). One key result from our program is the detection of CO emission from the host galaxies of 8 quasars (Wang et al. 2010). High resolution imaging shows that the CO is centered within 0.2" of the quasar, at least in one source (Walter et al. 2004; Riechers et al. 2009), and CO almost certainly provides the host galaxy redshift to very high accuracy ($\Delta z < 0.002$). In parallel, we have been using near-IR spectra to detect MgII emission from $z \sim 6$ quasars (Kurk et al. 2007; Jiang et al. 2007), which also provides much more accurate host galaxy redshifts ($\Delta z \leq 0.007$).

2. The quasars and redshifts

We have assembled a sample of 27 $z \sim 6$ quasars, all of which have reasonable signal-to-noise rest-frame UV spectra required for this analysis, mostly from the Keck telescope. Most of these (24) are from the Sloan Digital Sky Survey from Fan et al. (2006c) and Jiang et al. (2008). J1425+3254 was discovered in the AGN and Galaxy Evolution Survey of Cool et al. (2006). J2329-0301 and J1509-1749 are from the Canada-France High-z Quasar Survey of Willott et al. (2007). Eight of this sample are detected in CO, from which an accurate z_Q is derived (see Wang et al. 2010 and references therein). Nine of the sources have z_Q measured from the MgII emission line (Kurk et al. 2007; Jiang et al. 2007). The other ten objects have redshifts determined from the Lyα+NV lines.

We summarize all the parameters in Table 1, including the quasar 1450 $\mathring{A}$ absolute magnitude (M_{1450}), redshifts, and comoving radial distances[2].

We adopt the definition of the NZ radius (R_{NZ}) used in Fan et al. (2006b), i.e. the physical distance implied by the Hubble flow, derived from the difference between the quasar host galaxy redshift (z_Q) to the point (z_{GP}) where the transmitted flux first drops by a statistically significant amount to below 10% of the quasar extrapolated continuum emission: $R_{p,NZ} = (D_Q - D_{GP})/(1 + z_Q)$, after the spectrum is smoothed to a resolution of $20\mathring{A}$. D_Q and D_{GP} are the co-moving distances implied by the redshifts. Following Fan et al. (2006b), we fit a double Gaussian + power-law profile to the quasar spectrum redward of Lyα as the quasar intrinsic continuum and then calculate transmitted flux as a function of wavelength.

Spectra of the SDSS quasars are from Fan et al. 2006 and Jiang et al. 2008. The spectrum of the AGES quasar (J1425+3254) is from Cool et al. (2006). For the two Willott et al. quasars, J2329-0301 and J1509-1749, we have not re-fit the spectra, but use the $R_{p,NZ}$ values quoted in Willott et al. (2007). Again, to be consistent with the sample in Table 1, we adopt the strict definition of Fan et al. (2006) of R_{NZ} defined by the first redshift (below the quasar redshift) at which the transmission drops below 0.1.

To properly compare NZ sizes, we normalize all the $R_{p,NZ}$ values to a fixed UV absolute magnitude $M_{1450} = -27$, using the relation: $R_{NZ,corrected} = R_{p,NZ} \times 10^{0.4(27+M_{1450})/3}$. The $R_{NZ,corrected}$ values are listed in the last column of Table 1.

Three sources in Table 1, J0353+0104, J1044-0125, and J1048+4637, are broad absorption line (BAL) quasars (Fan et al. 2006c; Jiang et al. 2008), and the source J1335+3533

[2]Ned Wright's cosmological code is used in the calculation (Wright 2006) with the standard WMAP cosmology (Spergel et al. 2007).

has a lineless UV spectrum discovered in Fan et al. (2006c). For completeness, we calculate the R_{NZ} values for these quasars in Table 1. However, as with Fan et al. (2006b), we exclude these quasars from our subsequent analysis due to the fundamentally different nature of their intrinsic spectra, in particular around the Lyα emission redshift. The different intrinsic spectra imply that using the same spectral fitting analysis technique described above to derive z_{GP} could lead to erroneous results. Keeping this cautionary note in mind, it is interesting that these sources are all among the smallest near-zones in the sample, and three of the four have been detected in CO. The presence of a BAL, and of CO in the host galaxy, implies relatively dense local environments for these quasars, and hence larger UV attenuation, which could lead to small R_{NZ} values.

3. Redshift errors

The Lyα+NV redshifts have large uncertainties of $\Delta z \sim 0.02$, due to emission broad line widths, Gunn-Peterson absorption, and offsets between different ionization lines in quasar spectra (Richards et al. 2002, 2003; Fan et al. 2006c). This implies an uncertainty of $\Delta R_{NZ} \sim 1.2$ Mpc. There is also a systematic offset of similar magnitude between the MgII and higher ionization broad line redshifts (Richards et al. 2002). We have corrected the redshifts in the bottom section of Table 1 ('other redshifts') using this mean offset (+0.02 in z; note that J2315-0023 was already corrected in the literature).

Richards et al. (2002) compare MgII broad line redshifts with [OIII] narrow line redshifts in lower z quasars and find: $z(MgII) - z([OIII]) = -97 \pm 269$ km s^{-1}. We add to this the uncertainties in spectral fitting ($\Delta z \sim 0.003$; Jiang et al. 2007; Kurk et al. 2007), and estimate a typical uncertainties in the MgII redshifts of $\Delta z \sim 0.007$, implying $\Delta R_{NZ} \sim 0.4$ Mpc. The CO observations significantly improve the redshift measurements, with an uncertainty of $\Delta z \leq 0.002$, implying $\Delta R_{NZ} \sim 0.1$ Mpc.

Considering the errors on z_{GP}, Fan et al. (2006b) estimate that at 20$\mathring{A}$ resolution, they can measure the onset of the Gunn-Peterson trough to an accuracy of at least 10$\mathring{A}$, or $\Delta z_{GP} \sim 0.01$. This is certainly a conservative estimate of the error, and implies $\Delta R_{NZ} \sim 0.6$ Mpc due to errors in z_{GP}. We add this error in quadrature to the errors on z_Q. The implied total errors are then: (i) $\Delta R_{NZ} = 1.34$Mpc (physical) for sources with Lyα redshifts, (ii) $\Delta R_{NZ} = 0.72$Mpc for sources with MgII redshifts, and (iii)$\Delta R_{NZ} = 0.60$Mpc for sources with CO redshifts.

4. Analysis

We plot the $R_{NZ,corrected}$ values versus quasar redshift in Figure 1. Again, we omit the three BAL sources and the lineless quasar from this analysis for reasons given in Section 2. The figure shows a decrease in R_{NZ} with increasing redshift. A weighted linear fit to the data points gives $R_{NZ,corrected} = (7.4 \pm 0.3) - (8.0 \pm 1.1) \times (z - 6)$, while an unweighted fit yields a similar result of $R_{NZ,corrected} = (7.7 \pm 0.4) - (6.8 \pm 2.1) \times (z - 6)$. The errors were computed both from the formal fitting process, as well as by computing the scatter in the fitted parameters after fitting realizations removing one data point at time. To be conservative, we adopt the larger errors from the latter process in the analysis below.

For the weighted fit, the mean NZ radius changes from 9.8 ± 0.9 Mpc at $z = 5.7$, to 4.2 ± 0.4 Mpc at $z = 6.4$. The Spearman rank correlation coefficient for the distribution is $\rho = -0.51$, implying a probability that there is no correlation between redshift and $R_{NZ,corrected}$ of just 1%. Further, a Student's t-test gives a probability of 1% for the hypothesis that the slope is zero (ie. no change in mean NZ size over this redshift range). In the simplest physical picture, $R_{NZ} \propto f(HI)^{-1/3}(1 + z_Q)^{-1}$, implying an increase in the volume averaged neutral fraction by a factor ~ 9.4 from $z = 5.7$ to 6.4.

After removing the linear slope in redshift, we calculate an rms for the scatter in the normalized NZ sizes of $\sigma_{NZ} = 2$ Mpc. Fan et al. (2006b) see a similar scatter, but could not say whether this was due to errors in z_Q or physical differences between quasars. In our sample, the measurement errors are all below this rms value, and hence there must be intrinsic physical differences between quasars, either in terms of their environments, or AGN properties (eg. quasar age, SED).

Figure 2 shows the mean absorption profiles in the quasar NZ for three different redshift bins. This is the updated version of Fig. 13 in Fan et al. (2006b), and as with Fan et al., we do not scale the profile according to the quasar luminosity in this case. There is a clear evolution in profiles. The lowest redshift bin first drops below 10% transimission by a statistically significant amount at 8.5 Mpc radius, while this occurs for the highest redshift bin at 3.5 Mpc. Fan et al. (2006b) point out that this marked difference in absorption profiles from $z \sim 5.85$ to $z > 6.15$ is a graphic illustration of the change in the mean neutral state of the IGM at $z \sim 6$.

Figure 3 shows the relationship between $R_{p,NZ}$ and M_{1450}. Figure 3a shows $R_{p,NZ}$ values taken directly from Table 1, and Figure 3b shows the values after normalizing-out the linear regression relationship between NZ size and redshift derived from Figure 1, which we designate as $R_{p,NZ,norm}$. A correlation is found between NZ sizes and M_{1450}. The Spearman rank correlation coefficient for the distribution in Figure 3b is $\rho = -0.57$, implying a prob-

ability that there is no correlation between M_{1450} and $R_{p,NZ,norm}$ of just 0.4%. Included in Figure 3 is a dotted line that follows the relationship: $R_{p,NZ} \propto \dot{N}_Q^{1/3}$, as naively expected for photo-ionization dominated by quasar radiation. This line has not been fit to the data, but is shown for reference. The overall trend of increasing $R_{p,NZ}$ with the quasar luminosity is consistent with this very simple model, although the scatter is such that this is by no means proof of the model.

As a final comparison, Figure 4 shows the relationship between M_{1450} and redshift. We find no correlation between quasar absolute magnitude and redshift over the narrow redshift range of this sample. Formally, the Spearman rank correlation coefficient for the distribution is $\rho = 0.11$, implying a high probability that there is no correlation between redshift and M_{1450} of 62%.

5. Discussion

Using a larger sample and improved quasar host redshifts, we have confirmed a statistically significant increase in luminosity normalized NZ sizes from $z \sim 6.4$ to 5.7, first noted by Fan et al. (2006b). In the simplest physical model, the factor 2.3 change in mean NZ radius is consistent with a factor of 9.4 decrease in mean neutral fraction from $z \sim 6.4$ to 5.7. Fan et al. (2006b) derive a volume averaged neutral fraction of 9.3×10^{-5} at $z = 5.7$ from their analysis of GP absorption troughs and gaps. The NZ measurements then suggest that the neutral fraction has increased to $\sim 9 \times 10^{-4}$ at $z = 6.4$.

Wyithe et al. (2008) and Bolton et al. (2010) have proposed an alternative interpretation for this evolution in NZ sizes. Based on numerical simulations, they argue that the dominant effect on quasar near-zones during the end of reionization, or the percolation stage, may be a rapidly increasing contribution to photo-ionization from the cosmic ionizing background with cosmic time. The increasing mean free path allows the background photons to contribute substantially to the ionization around the edge of the NZ, thereby effectively increasing the observed sizes of the NZ. In either case, the results are consistent with the idea that $z \sim 6$ to 7 corresponds to the tail end of cosmic reionization.

Our improved z_Q measurements imply that the intrinsic scatter in the NZ sizes is large at any given redshift: $\sigma_{NZ} = 2$ Mpc. This large scatter must reflect real physical differences between quasars, perhaps some combination of differences in SEDs, UV escape fractions, ages, and/or local environments. Bolton & Haehnelt (2007b) have argued that the quasar age is less a factor when f(HI) < 0.1, since the size is then most likely dictated by absorption (and recombination) in denser regions of residual neutral gas within the sphere itself. The

small NZ sizes seen for the BAL quasars in Table 1 suggest a dependence on the immediate local environment, although see the cautionary note in Section 2 concerning these sources.

We also find an increase in $R_{p,NZ}$ with quasar UV luminosity. This correlation is qualitatively consistent with photo-ionization dominated by quasar radiation. Lastly, we find no correlation between M_{1450} and redshift over the relatively narrow redshift range explored in this sample.

We re-emphasize that the use of the near-zone technique has major pit-falls when trying to estimate the absolute neutral fraction at a given redshift, as detailed in Fan et al. (2006b) and Bolton & Heahnelt (2007a,b). In this paper, we have improved substantially one of the observational uncertainties in the calculation, namely, the quasar host galaxy redshifts, and we have focused on the evolution of the NZ sizes and neutral fraction, not the absolute neutral fraction. Still, as Bolton & Heahnelt point out, a larger sample with accurate measurements of the spectral regions around both Lyα and Lyβ is necessary to set meaningful constraints on the absolute neutral fraction of the IGM using the NZ technique.

CC thanks the Max-Planck-Gesellschaft and the Humboldt-Stiftung for support through the Max-Planck-Forschungspreis, and the Max-Planck Institute for Astronomie in Heidelberg for their hospitality. The authors thank J. Bolton, S. Wyithe, C. Willott, and the referee for useful comments. DR acknowledges support from NASA through Hubble Fellowship grant HST-HF-51235.01 awarded by the STScI, operated by AURA for NASA, under contract NAS 5-26555.

Bertoldi, F., Cox, P., Neri, R. 2003, A& AL, 409, L47

Bertoldi, F., Carilli, C., Cox, P. 2003, A& AL, 406, L55

Bolton, J. & Haehnelt, M. 2007a, MNRAS, 374, 493

Bolton, J. & Haehnelt, M. 2007b, MNRAS, 381, L35

Bolton, J., Becker, G., Wyithe, J.S. et al. 2010, MNRAS, in press (arXiv:1001.3415)

Carilli, C., Neri, R., Wang, R. et al. 2007, ApJL, 666, L9

Cen, R. & Haiman, Z., 2000, ApJ, 542, L74

Fan, X., Carilli, C., Keating, B. 2006a, ARAA, 44, 415

Fan, X, Strauss, M., Becker, R. et al. 2006b, AJ, 132, 117

Fan, X, Strauss, M., Richards, G. et al. 2006c, AJ, 131, 1203

Fan, X, Strauss, M., Becker, R. et al. 2002, 123, 1247

Fan, X, et al. 2003, AJ, 125, 1649

Furlanetto, S.R. , Hernquist, L. & Zaldarriaga, M. 2004, MNRAS, 354, 695

Gnedin, N. Y. 2004, ApJ, 610, 9

Gnedin, N.Y., Prada, F. 2004, ApJ, 608, L77

Gunn, J. E. & Peterson, B. A. 1965, ApJ, 142, 1633

Haiman, Z. 2002, ApJ, 576, L1

Jiang, L., Fan, X., Vestergaard, M. et al. 2007, AJ, 134, 1150

Komatsu, E., Smith, K., Dunkley, J. et al. 2010, ApJS, in press (arXiv:1001.4538)

Kurk, J., Walter, F., Fan, X. et al. 2007, ApJ, 669, 32

Lidz, A., McQuinn, M., Zaldarriaga, M., Hernquist, L., Dutta, S. 2007, ApJ, 670, L39

Madau, P., Rees, M.J., 2000, ApJ, 542, L69

Maselli, A., Gallerani, S., Ferrara, A., Choudhury, T. 2007, MNRAS, 376, L34

Mesinger, A. & Haiman, Z. 2004, ApJ, 611, L69

Mesinger, A. 2010, MNRAS, in press (arXiv:0910.4161)

Richards, G.T., et al., 2002, AJ, 124, 1

———————. 2003, Astron.J., 127, 1305

Riechers, D., Walter, F., Bertoldi, F. et al. 2009, ApJ, 703, 1338

Shapiro, P. & Giroux, M. 1987, ApJL, 321, 107

Spergel, D., Bean, R., Dore, O., et al. 2007, ApJS, 170, 377

Walter, F., Bertoldi, F., Carilli, C.L. et al., 2003, Nature, 424, 406

Walter, F., Carilli, C., Bertoldi, F., Menten, K., Cox, P., Lo, K.Y., Fan, X., Strauss, M., 2004, ApJ, 615, L17

Walter, F., Riechers, D., Cox, P. et al. 2009, Nature, 457, 699

Wang, R., Carilli, C.L., Wagg, J. et al. 2010, ApJ, submitted

Wang, R., Carilli, C.L., Wagg, J. et al. 2008, ApJ, 687, 848

Wang, R., Carilli, C.L., Beelen, A. et al. 2007, AJ, 134, 617

White, R., Becker, R., Fan, X., Strauss, M. 2003, AJ, 126, 1

White, R., Becker, R., Fan, X., Strauss, M. 2005, AJ, 129, 2102

Willott, C.J., Delorme, P., Reyle, C. et al. 2009, arXiv:0912.0281

Willott, C.J., Delorme, P., Omont, A., et al. 2007, AJ, 134, 2435

Wright, E. 2006, PASP, 118, 1711

Wyithe, J. S. B. & Loeb, A. 2004, ApJ, 612, 597

Wyithe, J.S., Loeb, A., Carilli, C. 2005, ApJ, 628, 575

Wyithe, J.S., Bolton, J., Haehnelt, M. 2008, MNRAS, 383, 691

Yu, Q., Lu, Y. 2004, ApJ, 602, 603

Table 1: Redshifts, comoving distances, and proper NZ radii

Name	M_{1450}	z_Q	D_Q Mpc	z^b_{GP}	D_{GP} Mpc	$R^c_{p,NZ}$ Mpc	$R_{NZ,corrected}$ Mpc
CO redshifts[a]							
J084035.0+562419	-26.66	5.8441	8352.6	5.69	8281.8	10.4	11.5
J092721.8+200123	-26.78	5.7722	8319.9	5.70	8286.5	4.9	5.3
J104433.0−012502[d]	-27.47	5.7824	8324.5	5.70	8286.5	5.7	4.9
J104845.0+463718[d]	-27.55	6.2284	8519.2	6.16	8490.5	4.0	3.4
J114816.6+525150	-27.82	6.4189	8596.9	6.33	8561.0	4.9	3.8
J133550.8+353315[d]	-26.82	5.9012	8378.2	5.89	8373.2	0.76	0.8
J142516.3+325409	-26.09	5.8918	8374.0	5.76	8314.3	8.8	11.6
J205406.4−000514	-26.15	6.0379	8438.3	5.97	8408.7	4.2	5.5
Mg II redshifts[e]							
J000552.3−000655	-25.87	5.850	8355.2	5.77	8318.9	5.3	7.5
J030331.4−001912	-25.48	6.078	8455.6	6.00	8422.2	4.7	7.5
J083643.8+005453	-27.88	5.810	8337.1	5.62	8248.9	13.0	9.9
J103027.1+052455	-27.16	6.308	8552.0	6.21	8511.5	5.6	5.3
J130608.2+035626	-27.19	6.016	8428.8	5.92	8386.6	6.0	5.7
J141111.2+121737	-26.74	5.904	8379.5	5.82	8341.7	5.4	5.9
J150941.7−174926	-26.98	6.118	–	–	–	4.3	4.3
J162331.8+311200	-26.67	6.247	8526.9	6.16	8490.5	5.1	5.6
J163033.9+401209	-26.12	6.065	8450.0	5.94	8395.4	7.7	10.1
Other Redshifts[f]							
J000239.3+255034	-27.67	5.82	8341.7	5.65	8263.1	11.5	9.4
J035349.7+010404[d]	-26.53	6.049	8443.1	6.02	8430.5	1.8	2.1
J081827.4+172251	-27.40	6.02	8430.5	5.89	8373.2	8.1	7.2
J084119.5+290504	-27.12	5.98	8413.0	5.81	8337.1	10.9	10.5
J113717.7+354956	-27.12	6.03	8434.9	5.91	8382.1	7.5	7.2
J125051.9+313021	-27.14	6.15	8486.3	6.03	8434.9	7.2	6.9
J143611.7+500706	-26.54	5.85	8355.2	5.72	8295.8	8.7	10.0
J160253.9+422824	-26.83	6.09	8460.7	5.94	8395.4	9.2	9.7
J231546.5−002358	-25.43	6.117	8472.3	6.05	8443.5	4.1	6.6
J232908.2−030158	-25.23	6.427	–	–	–	3.7	6.4

[a]Errors on z_Q based on CO redshifts are $\Delta z \sim 0.002$.

[b]Errors on z_{GP} at 20$\AA$ resolution estimated by Fan et al. (2006b) are $\Delta z \sim 0.01$.

[c]In section 3, we estimate errors in $R_{p,NZ}$ as: $\Delta R_{p,NZ} = 1.34$ Mpc for sources with Lyα redshifts, 0.72 Mpc for sources with MgII redshifts, and 0.60 Mpc for sources with CO redshifts.

[d]BAL or lineless quarsar, see Section 2.

[e]Errors on z_Q based on MgII redshifts are $\Delta z \sim 0.007$.

[f]Errors on z_Q based on Lyα+NV redshifts are $\Delta z \sim 0.02$.

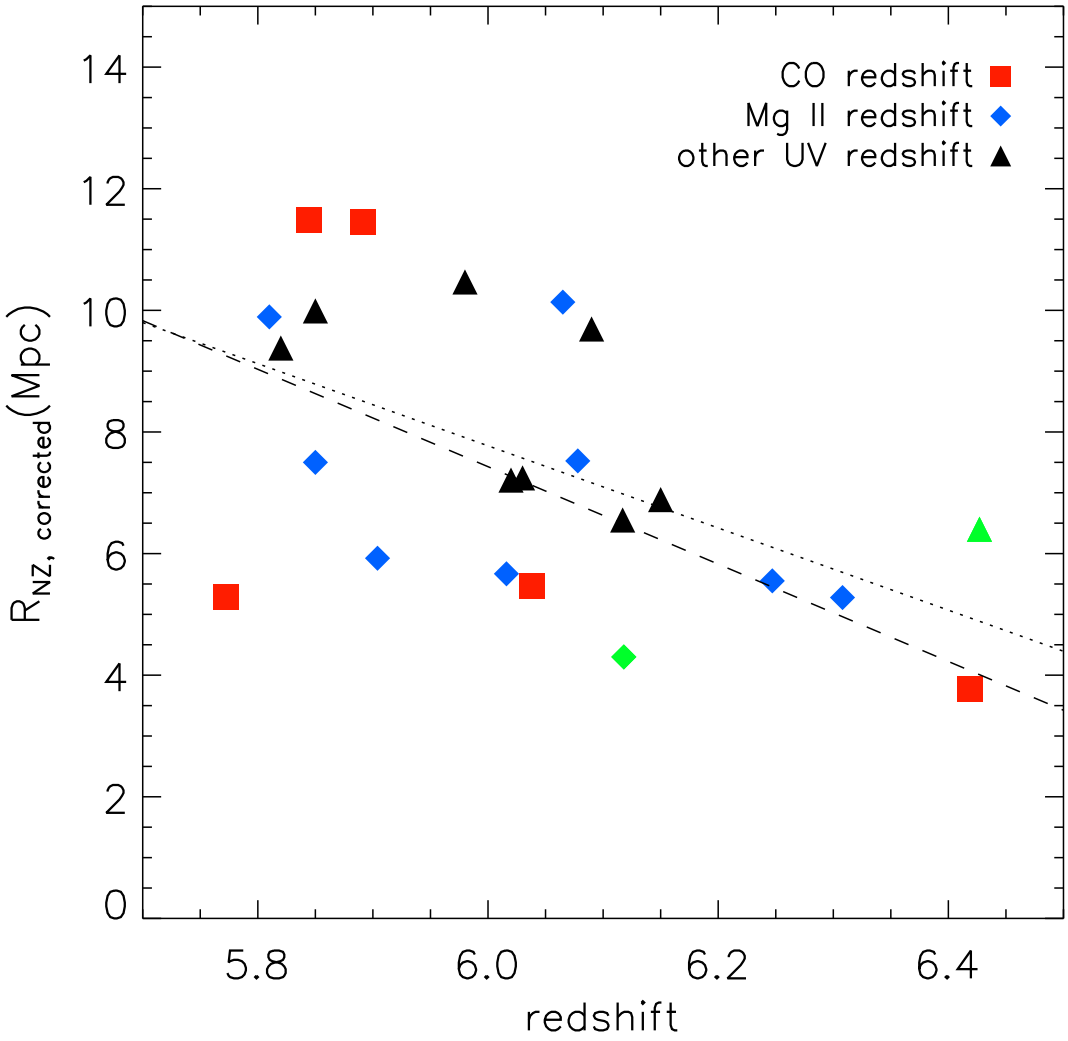


Fig. 1.— Radii of the luminosity normalized cosmological Strömgren spheres ($R_{NZ,corrected}$) around the z∼6 quasars versus their redshifts. Data are from Table 1, and again, we omit the three BAL sources and the lineless quasar from this plot and analysis for reasons given in Section 2. The red squares represent the sources which have CO redshifts. The blue diamonds represent sources with redshifts determined with Mg II λ 2798Å line emission, and the black triangles denote sources with redshifts determined with other UV lines from the discovery papers, such as Lyα + NV (see Fan et al. 2006b,c and references therein; Jiang et al. 2008). The errors for the different data points are: $\Delta R_{NZ,corrected}$ = 1.34 Mpc, 0.72 Mpc, and 0.60 Mpc, for the UV, MgII, and CO-determined z_Q uncertainties, respectively, including the error in z_{GP} added in quadrature. The long dash line show a weighted linear fit to the data with $R_{NZ,corrected} = (7.4 \pm 0.3) - (8.0 \pm 1.1) \times (z - 6)$. The dotted line shows an unwieghted fit. The two quasars from Willott et al. (2008) are shown in green, with the $R_{NZ,corrected}$ taken directly from that paper.

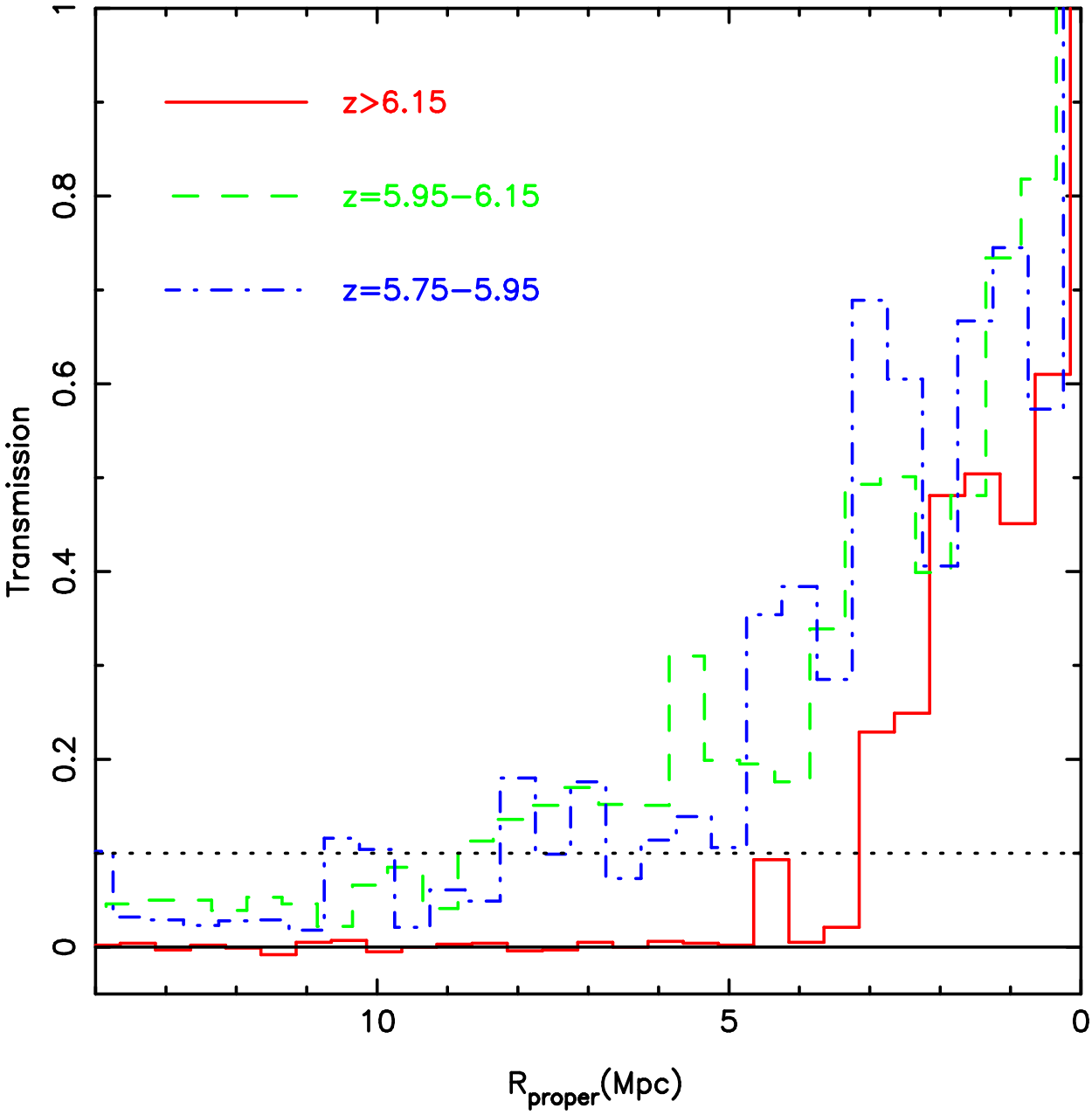


Fig. 2.— Average absorption profiles in the quasar near-zone for quasars in three different redshift bins: $z = 5.75 - 5.95$, $z = 5.95 - 6.15$ and $z > 6.15$. The Lyα+NV emission profile has been fitted with a Gaussian and removed. Note that the two Willott et al. quasars are not included in this plot.

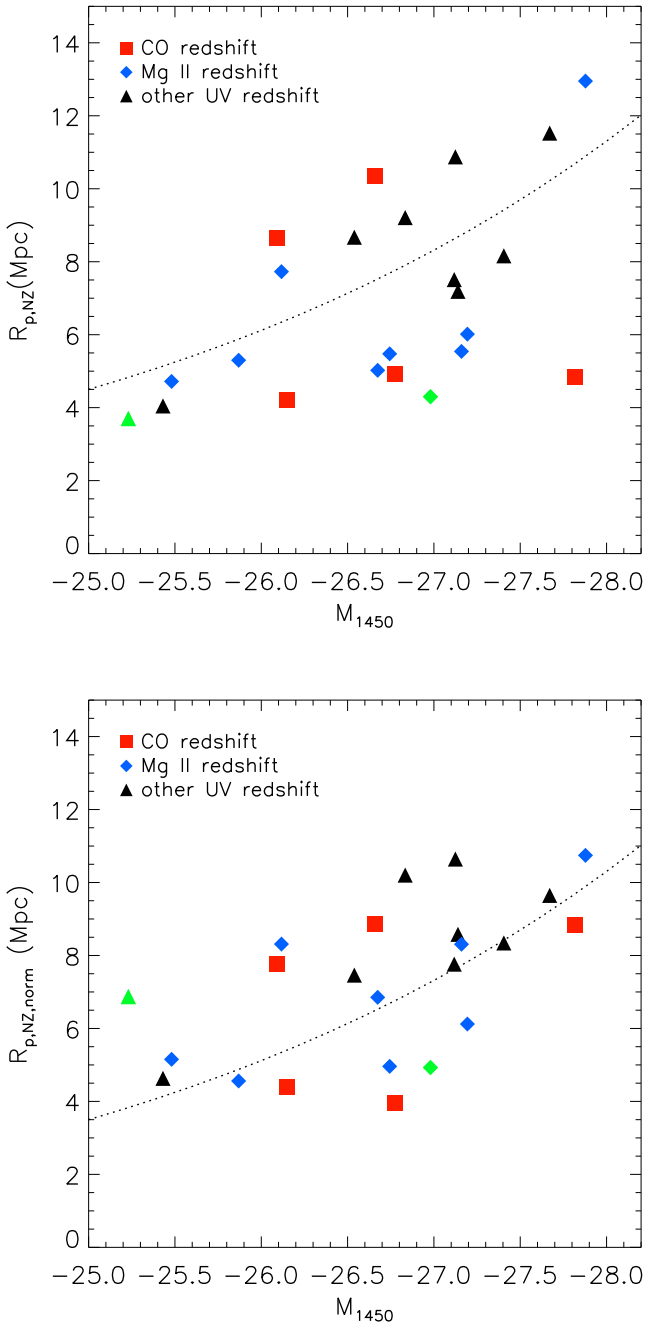


Fig. 3.— The relationship between $R_{p,NZ}$ and M_{1450}. The upper panel shows the values of $R_{p,NZ}$ as given in Table 1. The lower panel shows these same values with the linear relationship between redshift and NZ size derived from Figure 1 normalized-out. The dotted line is not a fit to the data, but shows the relationship: $R_{NZ} \propto \dot{N}_Q^{1/3} \propto 10^{-M_{1450}/7.5}$, as expected for photo-ionization dominated by quasar radiation. The scaling for this curve is arbitrary. The symbols are the same as in Figure 1.

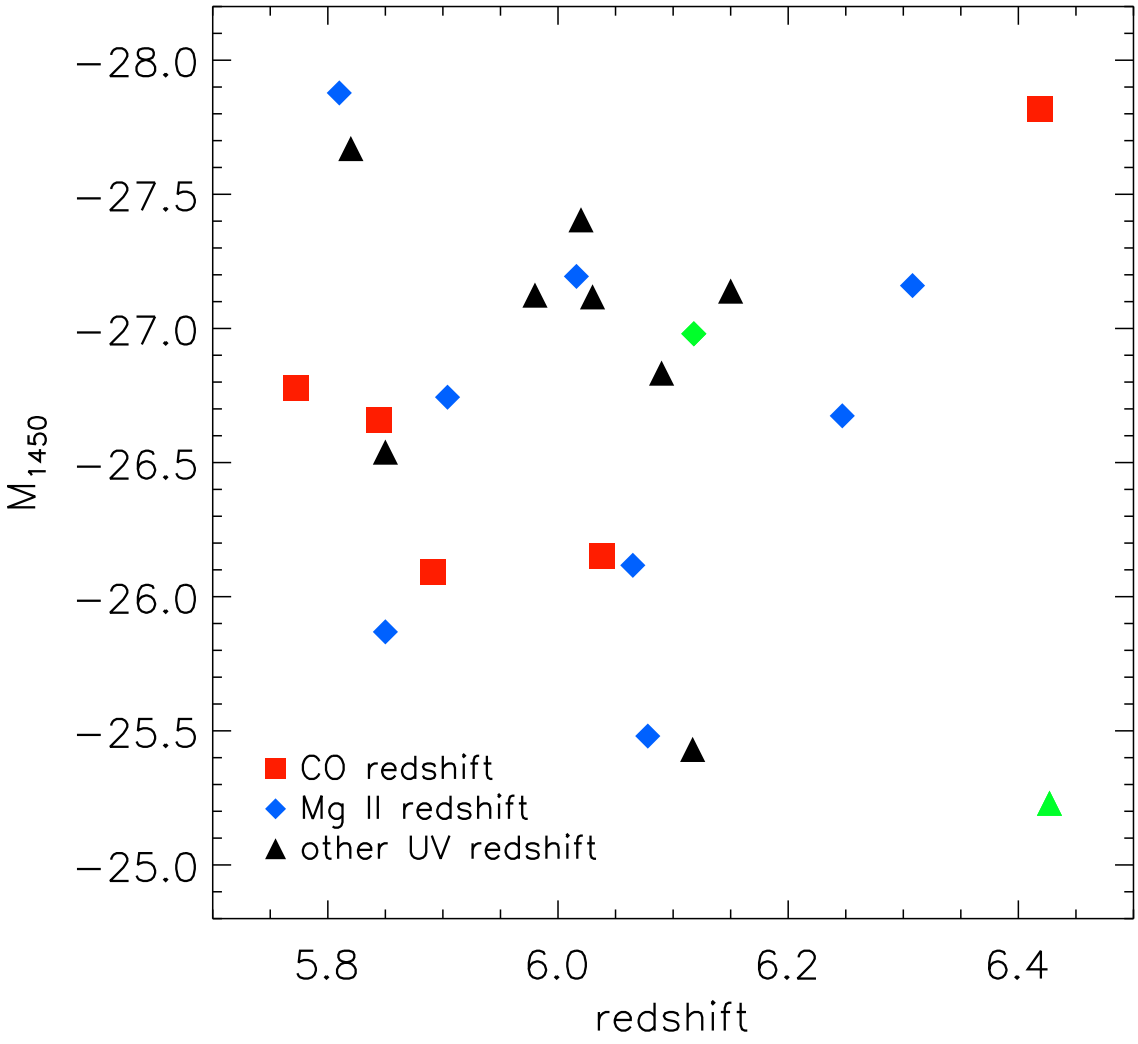


Fig. 4.— The relationship between redshift and M_{1450}. The symbols are the same as in Figure 1.